Received: 22 May 2024 | Revised: 9 August 2024 | Accepted: 9 September 2024 | Published online: 14 September 2024

RESEARCH ARTICLE

Journal of Optics and Photonics Research
2024, Vol. 00(00) 1–7
DOI: 10.47852/bonviewJOPR42023470

BON VIEW PUBLISHING

Study of Dependence of the Energy of the Field in Weakly Conductive Fiberlight-Guide with Gradient Refractive Index Profile Without Regard to Polarization

Victor D. Vlasenko[1],* and Vyacheslav A. Gladkikh[1]

[1]*Computing Center of the Far Eastern Branch of the Russian Academy of Sciences, Russia*

Abstract: A round-in-cross-section weakly guiding fiber optic light guide is considered. The system of Maxwellian equations for electrically conductive transparent media without due regard to polarization with an index of refraction in the case under consideration is reduced to the homogeneous Helmholtz equation, a particular solution of which is found using the Green's function. For a unimodalmode, a common decision was obtained for the field and energy inside the fiber in the general case of a gradient refractive index profile depending on the radial coordinate. The concept of normalized energy is introduced as the ratio of the energy inside a fiber with gradient refractive index profile to the energy inside a fiber with a step-index profile. Since in a single-mode regime the zero-order Bessel function, which describes the field inside a step-index profile fiber, can be replaced by a Gaussoid, then, when extending this replacement to the case of a single-mode gradient fiber, as a first approximation we shall obtain a finite expression for the normalized energy for a general gradient profile. The dependences of the normalized energy on the waveguide number were obtained for each of the degrees from the first to the fourth inclusive. It is shown that in the considered approximation, the energy increases up to a certain parameter values (for the first degree – a triangle profile) or slowly decreases (other profiles), after this value the energy increases for all profiles. The results obtained will help to select a suitable single-mode fiber for practical application.

Keywords: fiber light guide, optical fiber, single-mode regime, the Green's function, refractive index, polarization

1. Introduction

Science and technology have long used optical fiber (light guides), through which optical rays can propagate. The most common are well-studied fibers with stepped refractive index, and to a lesser extent, graded-index profile fibers are studied.

Due to the huge range of applications of optical fibers, extensive and mainly experimental research is being conducted to find optimal fiber materials for various purposes. The analytical study of waveguides has been well studied for step-index fibers. The studies in respect of a graded-index profile become more complicated due to the difficult problem of solving rather complex equations arising from the spatial dependence of the refractive index profile. Experimental studies have shown that a good model for the mathematical study of physical processes with a gradient profile can be a model of a power-law profile. The most famous precise solution is related to an unconstrained parabolic refractive index profile. Due to the difficulty of obtaining precise solutions for other cases of gradient profiles, various approximate methods are being developed for solving such equations.

Snyder and Love [1] can serve as a kind of encyclopedia, which widely represents quite extensive information about various types of optical waveguides with a brief description of both experimental and theoretical results with a large number of examples, and various mathematical methods known at the time of writing the book. Information about optical waveguides and dielectric waveguides is available in monographs [2–4]. However, the time has long passed since publication of these works, and research on this topic has advanced significantly. We shall briefly note these directions.

Brientin et al. [5] present a discussion of a multimode fiber optic device based on Fresnel reflection at the fiber end. When measured with Fresnel sensors using single-mode and multimode fibers, the differences in refractive indices are consistent with the values obtained from statistical studies.

In [6], a fiber with multichannel core and gradient refractive index in the shell is proposed. The fiber has low bending loss due to low refractive index grooves in the shell. Compared with the stepped ring, the refractive index gradient ring can also provide a larger mode area, in addition, it also fosters the enhancement of the bending resistance. To reduce cross-interference in space-division multiplexing fiber, paper [7] proposed a novel fiber with a composite index profile and dual auxiliary structure. The properties of such structure are significantly better than those of existing optical fibers, which promises broad prospects for use in high-capacity optical communication systems.

Henneking et al. [8] provide modeling of a 3D Petrov-Galerkin finite element model for simulating laser amplification in a fiber

*Corresponding author: Victor D. Vlasenko, Computing Center of the Far Eastern Branch of the Russian Academy of Sciences, Russia. Email: vlasenko@as.khb.ru

amplifier. Zhang et al. [9] propose a new method for quick refractive index measurement of single-mode stepped index fiber based on radially offset optical power scanning.

In the past few years, magneto-optical glasses have gained popularity due to their diverse applications. In [10], the nonlinear refractive index of a new magneto-optical glass formed in textured and optical fibers was studied. This result is relevant for expanding knowledge about magneto-optical materials. Talukdar et al. [11] discuss corrugated waveguides (waveguides in which the guide layer mainly consists of a plate with a strip or several strips applied upon).

Noteworthy is worked [12], where promising microstructures or holey fiber light guides made of quartz were first proposed – in the cladding of such light guides there are longitudinal holes made that are located in the cross-section relative to each other in one or another order. The large difference between the refractive indices of the core and cladding reveals the special optical properties of such waveguides. In particular, by changing the geometry of the cladding, it is possible to control the dispersion properties of the light guides. The mathematical apparatus for analyzing such fibers can be found in [13].

Dai et al. [14] carried out a comprehensive study of the characteristics of the output supercontinuum beam generated in a gradient multimode fiber and their relationship with the refractive index profile of the core. The simulation results provide good direction for improving the quality of the external supercontinuum produced by graded refractive multimode fiber.

A special task for the creation of condition monitoring systems for devices is the reliable measurement of deformation in various areas of the controlled structure. Fiber optic sensors are very good for solving such a task. The paper [15] presents the results of measuring deformations in zones of uniform and gradient distribution of deformations using fiber optic sensors based on Bragg gratings and distributed fiber optic sensors based on Rayleigh backscattering.

Bado et al. [16] present a work that aimed to introduce the readers to various techniques for deploying distributed optical fiber sensors (DOFS) for structural health monitoring (SHM) purposes. By collecting the most recent advances and findings on such DOFS SHM integrations, the authors contributed to the goal of collective growth toward effective SHM. Jayawickrema et al. [17] draw attention to the fact that structural health monitoring (SHM) systems in civil engineering system are becoming a subject of great attention by scientists and experimenters. In recent years, the technology of fiber optic devices has developed rapidly and various types of sensors have found practical applications in civil engineering.

The article [18] presents a method for detecting the occurrence and development of local damages in a material. It is based on experimental strain values measured by a limited number of sensors and the results of numerical modeling of the stress-strain state. Fiber optic sensors using Bragg gratings were used to measure deformation. The conducted experiments demonstrated the possibility of detecting damage based on the presented model. Wijaya et al. [19] review distributed fiber optic sensor technologies and their application ideas for large infrastructure health monitoring. The basic principle of distributed fiber optic sensor technology is presented. Examples of infrastructure monitoring are also discussed. In recent years, SHM has become an important direction in the development of large-scale civil engineering. The development and application of fiber optic sensing technology in the field of SHM is becoming more and more stable. This is the subject of paper [20].

Optical fibers that support multimode light guidance are an effective way to increase the capacity of an optical telecommunication network. Pereira et al. [21] investigate the possibility of introducing electro-optical mode interference steering in a few-mode fiber using a voltage applied to the internal electrodes of the fiber.

For those who study optics, physics, electrical engineering, and electronics, as well as for practitioners in related fields such as material science and chemistry, the fourth edition of the well-known manual [22] will be very useful. Monograph [23] discusses optical communications from a Fourier perspective. The sections are devoted to wave propagation in optical waveguides based on Maxwell's equations and nonlinear Schrödinger equation. It discusses the optical Fourier transform as a time lens, such as modulation format conversion and spectral amplification, and also discusses couplers and their use for optical discrete Fourier transform. Some provisions of the theory are more widely applicable beyond optical communications and are also important for the development of communication means. The book section on Fourier theory introduces the relationship between Fourier series and Fourier integral, as well as the associated Laplace transform.

The review [24] presents the manufacturing methods and applications of fiber optic devices based on the core-bias structure. First, the classification and manufacturing methods of the sensors are presented. Then, the application areas of different types of sensors are considered. Compared with traditional sensors, the sensor with a non-axisymmetric core-bias structure has very good sensitivity characteristics. The article [25] studies the dispersion of optical vortices in twisted elliptical fibers with torsional mechanical stresses. Based on the spectra of vortex modes of twisted elliptical fibers with step and gradient profiles, analytical expressions for polarization, topological, and hybrid types of dispersion of optical vortices are established.

Polyakova et al. [26] studied the problem of improving the characteristics of fiber optic measuring devices determined by the mechanical reliability of a bent optical fiber. The dependence of the luminous flux intensity on the change in the bending radius of an optical fiber is established. A new method for calculating an optical fiber is considered in [27]. The issue of extending the principles of circuit theory to elements with dispersed elements, i.e., optical fiber, is studied. Zhang et al. [28] studied the high-temperature connection of two types of optical fibers – an antiresonance hollow-core fiber and a fiber with a solid core ensuring low loss during the passage of laser radiation; for the study, it uses a bridge in the form of a refractive index gradient fiber, one end of which is connected to a hallow core fiber and the other to a solid core fiber. When the bridge is precisely cut along its length and its parameters are respectively changed, the required conversion of optical radiation passing through it from single-mode to multimode corresponding to the mode characteristics of a solid core fiber is achieved.

Optical fiber bundles are widely used in various fields of fiber optics, despite the relatively low resolution of such devices. To solve this problem, materials with a high refractive index are used. The review [29] shows the use of sapphire fibers with a high refractive index for this purpose.

As for classical gradient fibers, so far, an exact solution for the field in the fiber has been obtained only in the case of an unbounded parabolic profile – generalized Laguerre polynomials in cylindrical coordinates or Gauss-Hermite functions in Cartesian coordinates. A detailed analysis of this solution can be found in the classical literature [30]. In publication [31], for an arbitrary gradient planar waveguide, mode solutions of the Helmholtz equation are obtained: the mode amplitude is presented in the form of an exponential with an indicator in the form of a Taylor series, the coefficients of which are found from recurrence relations. Simulations show that Mikaelian gradient microlenses and Maxwell "fisheye" can produce super-resolution images.

For a 3D graded-index light guide with a circular cross-section, in [32] we obtained an analytical expression for the field and energy in a single-mode regime inside a weakly conductive fiber with a power-law refractive index profile with an arbitrary degree (taking into account polarization) by solving the Helmholtz equations using the Green's function. A regression of energy on the waveguide number for the second and third powers of the refractive index profile of the expression was constructed. It was demonstrated that in the one-dimensional approximation, the energy increases with the waveguide parameter up to a certain value of the parameter, after which the increment values for the powers of n = 2 to n = 3 change places.

2. Equation for a Field in a Fiber with Gradient Refractive Index Profile

Let $\vec{e}(t,R)$, $\vec{h}(t,R)$ be the electric and magnetic elements of the electromagnetic field respectively (t – time, $R = (x, y, z)$ – coordinates). When separating a time-dependent part from the Maxwell's equations for dielectric media with the index of refraction $n^2(R)$, as a result of transformations for the electric component of electromagnetic field (likewise for a magnetic component), we will gain [1]:

$$\begin{aligned}\vec{e}(t,R) = \vec{E}(R)\exp(-i\omega t) \to \Delta\vec{E} + k^2 n^2 \vec{E} \\ = -\nabla_t\{[\vec{E}, \nabla_t(\ln(n^2))]\}\,,\end{aligned} \tag{1}$$

$$\nabla_t \equiv \partial/\partial x + \partial/\partial y,\ \ \Delta_t \equiv \partial^2/\partial x^2 + \partial^2/\partial y^2,$$

where $k = \omega/c$, ω – cyclic frequency, c – light speed. For a fiber (a core) of a gradient light guide $n^2 = n^2(r)$, $r = \sqrt{x^2+y^2}$, the field in the fiber also depends on r and propagates along the axis z. For the field $\vec{E}$, let us write

$$\vec{E}(R) = \vec{n}_z \exp(i\beta z)\exp(im\varphi)\,\mathrm{E}(r), \tag{2}$$

where $\vec{n}_z$, ω, β – respectively the normal vector, the distribution parameter, and the angle in the plane (x, y).

The case with a nonzero right part in (2) was considered in a first approximation in the work [32]. Disregarding in (1) the right part (not considering the polarization properties describe by terms, containing $\nabla\{\ln n^2\}$), let's move from the formulas (1), (2) to the scalar equation in polar coordinates for the fundamental mode ($m = 0$)

$$\frac{d^2\mathrm{E}(r)}{dr^2} + \frac{1}{r}\frac{d\mathrm{E}(r)}{dr} + \{k^2 n^2(r) - \beta^2\}\,\mathrm{E}(r) = 0\,. \tag{3}$$

The refractive index for a waveguide is usually written as follows (n_{co}^2, n_{cl}^2 – the refractive indices of fiber and shell, Δ – the profile height, ρ – the radius of a fiber that is round in diameter)

$$\begin{aligned} n^2(r) = \begin{cases} n_{co}^2[1 - 2\Delta h(r)]\,, & 0 \le r \le \rho, \\ n_{cl}^2\,, & r > \rho, \end{cases} \\ \Delta = \frac{n_{co}^2 - n_{cl}^2}{2n_{co}^2}\,, \quad \begin{matrix} h(0) \equiv 0, \\ h(\rho) \equiv 1. \end{matrix} \end{aligned} \tag{4}$$

The function $h(r)$ increases from 0 to 1, $0 \le r \le \rho$.

Inserting (4) in (3), let's write the results in the form of

$$\begin{aligned} &\frac{d^2\mathrm{E}(r)}{dr^2} + \frac{1}{r}\frac{\mathrm{E}(r)}{dr} + \chi_1^2\mathrm{E}(r) = -4\pi F(r)\,, \\ &F(r) \equiv -\frac{V^2}{4\pi\rho^2}h(r)\mathrm{E}(r)\,, \\ &\chi_1^2 \equiv k^2 n_{co}^2 - \beta^2 \end{aligned} \tag{5}$$

(here $V \equiv k\rho NA$ – the waveguide index, $NA \equiv \sqrt{n_{co}^2 - n_{cl}^2}$ – the numerical aperture).

3. The Solution of Equation

Let's take the Equation (5) in the original Cartesian coordinates

$$\left(\frac{\partial^2}{\partial x^2} + \frac{\partial^2}{\partial y^2} + \chi_1^2\right)\mathrm{E}(x,y) = -4\pi\,F(x,y). \tag{6}$$

Representing F as

$$F(x,y) = \iint dx^{/}dy^{/}\delta(x^{/} - x)\,\delta(y^{/} - y)F(x^{/}, y^{/}), \tag{7}$$

here $\delta(x)$ – the delta-function, let's find a particular solution of the inhomogeneous Helmholtz equation in the following form

$$\mathrm{E}(x,y) \equiv \iint dx^{/}dy^{/}\,G(x,y;x^{/},y^{/})\,F(x^{/},\ y^{/}), \tag{8}$$

Inserting (7) in (8) in (5), we come to the equation for the Green's function G

$$(\Delta_t + \chi_1^2)\,G(x,y;x^{/},y^{/}) = -4\pi\delta(x^{/} - x)\,\delta(y^{/} - y),$$

the solution to which is

$$G(x,y,x^{/},y^{/}) = i\pi H_0^{(1)}(\chi_1 r_{12}),\ \ r_{12} = \sqrt{(x - x^{/})^2 + (y - y^{/})^2}\,, \tag{9}$$

here $H_0^{(1)}(x)$ the Hankel function.

Inserting (9) in (8) and considering the formula (5), in the polar coordinates we receive

$$\mathrm{E}(r) = -(iV^2/4\rho^2)\int_0^{2\pi} d\varphi^{/}\int_0^{\rho} dr^{/}r^{/}H_0^{(1)}(\chi_1 r_{12})h(r^{/})\mathrm{E}(r^{/}). \tag{10}$$

Having used the expansion [33]

$$\begin{aligned} H_0^{(1)}(\chi_1 r_{12}) = H_0^{(1)}(\chi_1 r)J_0(\chi_1 r^{/}) \\ + 2\sum_{k=1}^{\infty} H_k^{(1)}(\chi_1 r)J_k(\chi_1 r^{/})\cos(k\varphi^{/}). \end{aligned}$$

where $H_k^{(1)}(x) = J_k(x) + iN_k(x)$– the Hankel function of the first kind of k-th order, $J_k(x)$ – the Bessel function of k-th order, $N_k(x)$ – the Neumann function of k-th order, for (10), we will receive

$$\mathrm{E}(r) = -(i\pi V^2/2\rho^2)H_0^{(1)}(\chi_1 r)\int_0^{\rho} dr' r' J_0(\chi_1 r')h(r')\,\mathrm{E}(r') \quad (11)$$

The solution of the Equation (6) without the right part (for the considered case of fundamental mode) has the form of

$$\mathrm{E}_0(r) = J_0(\chi_1 r). \quad (12)$$

Omitting the primes in (11), let's write the common decision E_{tot} in the form of

$$\mathrm{E}_{tot}(\gamma) = \mathrm{E}_0(\gamma) + \mathrm{E}(\gamma) = const\left\{J_0(\chi_1\rho\gamma) - \frac{i\pi}{2}H_0^{(1)}(\chi_1\rho\gamma)\Psi(\chi_1\rho)\right\},$$
$$\Psi(\chi_1\rho) \equiv V^2\int_0^1 J_0(\chi_1\rho\gamma)\,h(\gamma)\mathrm{E}(\gamma)\gamma d\gamma. \quad (13)$$

4. Finding First Iteration and Energy in Optic Fiber

Let be $W_0 \equiv const\int_0^{\rho} E_0^2(r)rdr = (\gamma \equiv r/\rho) = const\cdot\rho^2\int_0^1 E_0^2(\gamma)\gamma d\gamma$ the power of the radical mode inside the fiber with a step profile ($E_0(r)$ which is the solution (12) of Equation (6) without the right-hand side when passing to polar coordinates (r, φ) for $\varphi = 0$); similarly, let be $W_{tot} \equiv const\int_0^{\rho}|E_{tot}(r)|^2 rdr = (\gamma \equiv r/\rho) = const\cdot\rho^2\int_0^1|E_{tot}(\gamma)|^2\gamma\,d\gamma$ the transmitted energy inside the fiber with a gradient profile under consideration ($E_{tot}(r)$ is the field (13)). Since it is not the absolute values of physical quantities that matter, but the relative ones, we will define the relative dimensionless power quantity – the normalized energy W_{norm}, as the ratio of the transmitted energy inside the fiber to the power of the fundamental mode inside the fiber with a step profile.

Inserting to the right part Ψ from (13), E_0 from (12) instead of E, for the normalized energy W_{norm} we fin ($N_0(x)$ – the Neumann function of zero order)

$$W_{norm} \equiv \frac{\int_0^1|\mathrm{E}_{tot}(\gamma)|^2\gamma d\gamma}{\int_0^1\mathrm{E}_0^2(\gamma)\gamma d\gamma} = \frac{1}{\int_0^1 J_0^2(\chi_1\rho\gamma)\gamma d\gamma}\left\{\left[1+\frac{\pi^2}{4}\Psi^2(\chi_1\rho)\right]\int_0^1 J_0^2(\chi_1\rho\gamma)\gamma d\gamma + \right.$$
$$\left. + \frac{\pi^2}{4}\Psi^2(\chi_1\rho)\int_0^1 N_0^2(\chi_1\rho\gamma)\gamma d\gamma + \pi\Psi(\chi_1\rho)\int_0^1 J_0(\chi_1\rho\gamma)N_0(\chi_1\rho\gamma)\gamma d\gamma\right]; \quad (14)$$

$$\Psi(\chi_1\rho) = V^2\int_0^1 J_0^2(\chi_1\rho\gamma)h(\gamma)\gamma d\gamma. \quad (15)$$

Using the known formulas [33]:

$$\int Z_p^2(\chi_1\rho\gamma)\gamma d\gamma = \frac{\gamma^2}{2}\left\{Z_p^2(\chi_1\rho\gamma) - Z_{p-1}(\chi_1\rho\gamma)Z_{p+1}(\chi_1\rho\gamma)\right\},$$
$$Z_{-n}(z) = (-1)^n Z_n(z),$$
$$\{J_1(z), N_1(z)\} = -\left\{J_0'(z), N_0'(z)\right\},$$
$$Z_p'(z) = \frac{dZ_p(Z)}{dz},$$
$$\gamma\in(0,1) \to \left\{N_0(z), N_0'(z)\right\} \approx \frac{2}{\pi}\left(\ln\frac{z}{2} + C\right)\left\{J_0(z), J_0'(z)\right\} \quad (16)$$

(Z_p – any cylindrical function, C – constant Euler–Mascheroni, $C = 0.5772156649$, $n = 0, 1, 2, \ldots$), let's write for the integrals in (14)

$$\int_0^1 J_0^2(\chi_1\rho\gamma)\gamma d\gamma = 12\left\{J_0^2(\chi_1\rho) + J_0'^2(\chi_1\rho)\right\},$$

wherefrom

$$\int_0^1 N_0^2(\chi_1\rho\gamma)\gamma d\gamma = \frac{1}{2}\left\{N_0^2(\chi_1\rho) + N_0'^2(\chi_1\rho)\right\} \approx \frac{1}{2}\left\{J_0^2(\chi_1\rho) + J_0'^2(\chi_1\rho)\right\}\times$$
$$\times\frac{4}{\pi^2}(\ln(\chi_1\rho/2)+C)^2 = \frac{4}{\pi^2}(\ln(\chi_1\rho/2)+C)^2\int_0^1 J_0^2(\chi_1\rho\gamma)\gamma d\gamma;$$
$$\int_0^1 J_0(\chi_1\rho\gamma)N_0(\chi_1\rho\gamma)\gamma d\gamma \approx \frac{2}{\pi}\int_0^1 J_0^2(\chi_1\rho\gamma)(\ln(\chi_1\rho/2)+C)\,\gamma d\gamma =$$
$$= \frac{2}{\pi}(\ln(\chi_1\rho/2)+C)\int_0^1 J_0^2(\chi_1\rho\gamma)\gamma d\gamma + \frac{2}{\pi}I(\chi_1\rho),\ I(\chi_1\rho) \equiv \int_0^1 d\gamma\gamma J_0^2(\chi_1\rho\gamma)\ln\gamma. \quad (17)$$

Considering the last integral as the function from the parameter $\chi_1\rho$, we will receive

$$I(\chi_1\rho) = -14\{J_0^2(\chi_1\rho) + 2J_1^2(\chi_1\rho) - J_0(\chi_1\rho)J_2(\chi_1\rho)\}. \quad (18)$$

Inserting (17) and (18) in (14), we receive

$$W_{norm}(V) = 1 + \left\{\frac{\pi^2}{4} + \ln((\chi_1\rho/2)+C)^2\right\}\Psi^2(\chi_1\rho) +$$
$$+ 2(\ln(\chi_1\rho/2)+C)\Psi(\chi_1\rho)$$
$$- \frac{\{J_0^2(\chi_1\rho) + 2J_1^2(\chi_1\rho) - J_0(\chi_1\rho)J_2(\chi_1\rho)\}}{2\int_0^1 J_0^2(\chi_1\rho\gamma)\gamma d\gamma}\Psi(\chi_1\rho). \quad (19)$$

The Bessel function $J_0(\chi_1\rho\gamma)$, describing regime of a waveguide with a stepped profile, as it is known, can be replaced by the Gaussian function (r_0 – the mode spot radius):

$$J_0(\chi_1\rho\gamma) \to \exp\{-\alpha\gamma^2/2\},\ \alpha \equiv \rho^2/r_0^2, \quad (20)$$

and (see, [32, 34]):

$$r_0 \cong \frac{0.4\lambda}{NA} \to \alpha \equiv \frac{\rho^2}{r_0^2} \cong 0.16V^2.$$

As in [32], according to (20), let's now require that for two descriptions different in form, the energy flux through the cross-section be the same:

$$\int_0^1 J_0^2(\chi_1\rho\gamma)\gamma d\gamma \equiv \int_0^1 \exp(-\alpha\gamma^2)\gamma d\gamma = \frac{1}{2\alpha}\{1-\exp(-\alpha)\}. \quad (21)$$

Inserting in (19), we receive:

$$W_{norm}(V) = 1 + \left\{\frac{\pi^2}{4} + \left(\ln\frac{\chi_1\rho}{2} + C\right)^2\right\}\Psi^2(\chi_1\rho) + 2\left(\ln\frac{\chi_1\rho}{2} + C\right)\Psi(\chi_1\rho) - \frac{\alpha\{J_0^2(\chi_1\rho) + 2J_1^2(\chi_1\rho) - J_0(\chi_1\rho)J_2(\chi_1\rho)\}}{\{1-\exp(-\alpha)\}}\Psi(\chi_1\rho). \quad (22)$$

The formula (22) coincides in form with the formula (19) from [32], which is expected (the method of approximate solution is the same), but they differ in the content of the function $\Psi(\chi_1\rho)$.

Further, according to (16) and (20)

$$\int_0^1 J_0^2(\chi_1\rho\gamma)\,\gamma d\gamma = \frac{1}{2}\left\{J_0^2(\chi_1\rho\gamma) + \frac{1}{(\chi_1\rho)^2}\left[\frac{d}{d\gamma}J_0(\chi_1\rho\gamma)\right]^2\right\}_{\gamma=1} \approx \frac{1}{2}\left\{\exp(-\alpha\gamma^2) + \frac{1}{(\chi_1\rho)^2}\left[\frac{d}{d\gamma}\exp\left(-\frac{\alpha\gamma^2}{2}\right)\right]^2\right\}_{\gamma=1} = = \frac{1}{2}\left\{1 + \frac{\alpha^2}{(\chi_1\rho)^2}\right\}\exp(-\alpha).$$

Comparing to (21), we get an expression for $\chi_1\,\rho$

$$(\chi_1\rho)(V) \approx \left\{\frac{\alpha^3}{\exp\alpha - 1 - \alpha}\right\}^{1/2}, \quad \alpha = 0.16V^2. \quad (23)$$

Finally, we have computed the functions $\Psi(\chi_1\rho)$.

5. The Function $\Psi = \Psi_n$ for Power-Low Refractive Index Profile and Dependence of "Normalized" Energy from a Waveguide Parameter and Power-Low Profile Degree Index

According to (15), for the power-low profile we get ($n = 1, 2, 3, \ldots$):

$$h(\gamma) \equiv \gamma^n \to \Psi_n(\chi_1\rho) = V^2\int_0^1 J_0^2(\chi_1\rho\gamma)\gamma^{n+1}d\gamma \quad (24)$$

Since it is difficult to take integrals of this type $\int_0^1 J_0^2(\chi_1\rho\gamma)\gamma^k d\gamma$ for $k \geq 2$, then using expression (20) for (24), we can write under the integrals

$$h(\gamma) \equiv \gamma^n \to \Psi_n = \Psi_n(V) \approx V^2\int_0^1 \exp(-\alpha\gamma^2)\gamma^{n+1}d\gamma. \quad (25)$$

Having confined to the values $n = 1, 2, 3, 4$, we find

$$\Psi_1(V) = \frac{V^2}{4\alpha}\left\{\sqrt{\frac{\pi}{\alpha}}\Phi\left(\sqrt{\alpha}\right) - 2\exp(-\alpha)\right\}, \quad (26)$$

$$\Psi_2(V) = \frac{V^2}{2\alpha^2}\{1 - (1+\alpha)\exp(-\alpha)\}, \quad (27)$$

$$\Psi_3(V) = \frac{V^2}{8\alpha^2}\left\{3\sqrt{\frac{\pi}{\alpha}}\Phi\left(\sqrt{\alpha}\right) - 2(3+2\alpha)\exp(-\alpha)\right\}, \quad (28)$$

$$\Psi_4(V) = \frac{V^2}{2\alpha^3}\{2 - [\alpha^2 + 2(1+\alpha)]\exp(-\alpha)\}, \quad (29)$$

$$\Phi(x) \equiv \frac{2}{\sqrt{\pi}}\int_0^x \exp(-t^2)dt,$$

(function $\Phi(x)$ – the integral of error function). The formulas (22) – (29) solve the problem. The calculations lead to the following regression of energy $W_{norm}(V)$ on the waveguide parameter at various values of the number n (Figure 1).

Figure 1
Regression of the energy $W_{norm}(V)$ on the waveguide number V without taking into account polarization

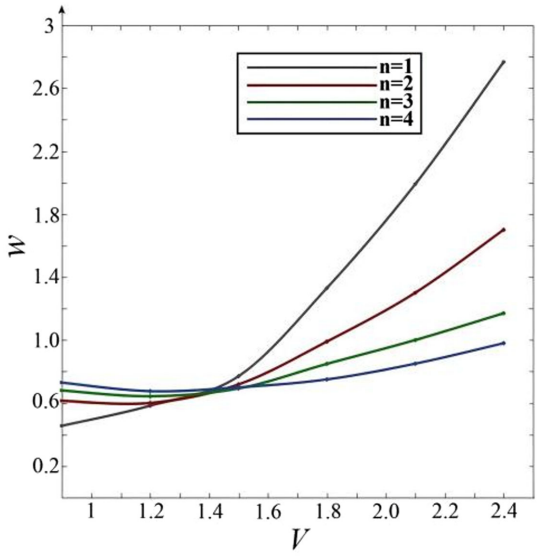

6. Conclusion

At a first approximation for a power-low profile with the values of the degrees $n = 1, 2, 3, 4$, there have been plotted the dependences of the energy $W_{norm}(V)$ on the waveguide number V. It is calculated that up to a value $V_c \approx 1.43$, the energy for the profile with $n = 1$ increases; for the profile with $n = 2$, it slowly decreases to $V \approx 1.2$ and then slowly increases up to V_c; for the profiles with $n = 3$ and $n = 4$, the energy slowly decreases to V_c. At $V > V_c$, the energy for the profiles increases, and here the triangle profile with $n = 1$ is energetically more advantageous than other profiles. The value $W_{norm}(V)$ reaches one at $V \approx 1.52$ *($n = 1$)*, at $V \approx 1.8$ *($n = 2$)*, and at $V \approx 2.4$ *($n = 3$)*, but for $n = 4$ the value $W_{norm}(V)$ does not reach one in the considered interval $V \in (0.9; 2.4)$. Here, we didn't take into account polarization effects (we solved the scalar equation). The accounting for these effects, earlier considered in the work [32] profiles with $n = 2$ and $n = 3$ (Figure 2), leads to a shift of V_c to the right – $V_c \approx 1.43 \to V_c = 1.55$, the rise being small for $n = 3$ and a more sharp rise for $n = 2$.

The results obtained in this work can be used in designing waveguides taking into account specific applications.

Figure 2
Dependence of the energy $W_{norm}(V)$ on the waveguide parameter V taking into account polarization

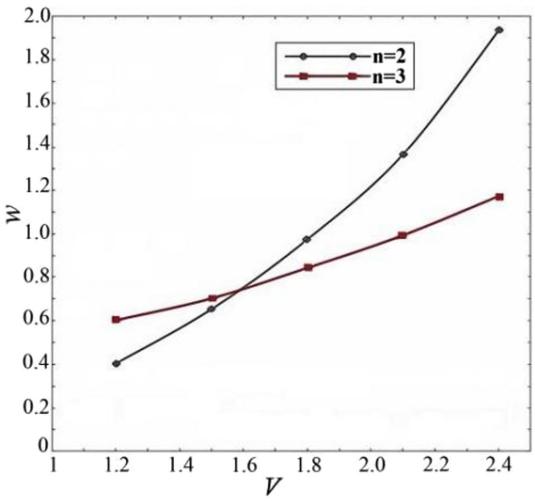

Ethical Statement

This study does not contain any studies with human or animal subjects performed by any of the authors.

Conflicts of Interest

The authors declare that they have no conflicts of interest to this work.

Data Availability Statement

Data are available from the corresponding author upon reasonable request.

Author Contribution Statement

Victor D. Vlasenko: Methodology, Software, Validation, Investigation, Writing – original draft, Writing – review & editing, Visualization. **Vyacheslav A. Gladkikh:** Conceptualization, Methodology, Validation, Formal analysis, Investigation, Writing – original draft.

References

[1] Snyder, A. W., & Love, J. D. (1983). *Optical waveguide theory*. UK: Chapman and Hall.

[2] Midwinter, J. E. (1979). *Optical fibers for transmission*. USA: John Wiley & Sons.

[3] Cheo, K. (1985). *Fiber optics: Devices and system*. USA: Prentice Hall.

[4] Okamoto, K. (2021). *Fundamentals of optical waveguides*. USA: Academic Press.

[5] Brientin, A., Leduca, D., Gaillarda, V., Girard, V., & Lupi, C. (2021). Numerical and experimental study of a multimode optical fiber sensor based on Fresnel reflection at the fiber tip for refractive index measurement. *Optics & Laser Technology*, *143*, 107315. https://doi.org/10.1016/j.optlastec.2021.107315

[6] Tong, Y., Chen, S., & Tian, H. (2018). A bend-resistant low bending loss and large mode area two-layer core single-mode fiber with gradient refractive index ring and multi-trench. *Optical Fiber Technology*, *45*, 235–243. https://doi.org/10.1016/j.yofte.2018.07.010

[7] Wang, G., Zhang, J., Zhang, H., Wang, F., Yan, X., Zhang, X., . . . , & Cheng, T. (2019). A low crosstalk multi-core few-mode fiber with composite refractive index profile and air-hole embedded trench assistance. *Optics Communications*, *499*, 127258. https://doi.org/10.1016/j.optcom.2021.127258

[8] Henneking, S., Grosek, J., & Demkowicz, L. (2021) Model and computational advancements to full vectorial Maxwell model for studying fiber amplifiers. *Computers & Mathematics with Applications*, *85*(1), 30–41. https://doi.org/10.1016/j.camwa.2021.01.006

[9] Zhang, S., Guo, H., Liu, X., Wang, P., Wang, Z., & Liu, Y. G. (2023). A simple refractive index measurement method for step-index fiber based on radial displacement optical power scan. *Optics Communications*, *544*, 129628. https://doi.org/10.1016/j.optcom.2023.129628

[10] Henrique, F. R., Pelosi, A. G., Almeida, J. M., Franco, D. F., Cocca, L. H., Nalin, M., . . . , & Mendonça, C. R. (2024). Nonlinear refraction in high terbium content borogermanate glass bulk and fiber. *Optical Materials*, *147*, 114635. https://doi.org/10.1016/j.optmat.2023.114635

[11] Talukdar, T. H., Allen, G. D., Kravchenko, I., & Ryckman, J. D. (2019). Single-mode porous silicon waveguide interferometers with unity confinement factors for ultra-sensitive surface adlayer sensing. *Optics Express*, *23*(16), 22485–22498. https://doi.org/10.1364/OE.27.022485

[12] Knight, J. C., Birks, T. A., Russell, P., St. J., & Atkin, D. M. (1996). All-silica single-mode optical fiber with photonic crystal cladding. *Optics Letters*, *21*(19), 1547–1549. https://doi.org/10.1364/OL.21.001547

[13] Sharma, D. K., Tripathi, S. M., & Sharma, A. (2019). Modal analysis of high-index core tellurite glass microstructured optical fibers in infrared regime. *Journal of Non-Crystalline Solids*, *511*, 147–160. https://doi.org/10.1016/j.jnoncrysol.2019.02.001

[14] Dai, J., Zhu, X., Zhang, B., & Hou, J. (2024). The influence of refractive index profile on supercontinuum beams self-cleaning in graded index multimode fiber. *Optics & Laser Technology*, *171*, 110454. https://doi.org/10.1016/j.optlastec.2023.110454

[15] Matveenko, V., Kosheleva, N., & Serovaev, G. (2023). Strain registration in the gradient zone by two types of fiber-optic sensors. *Procedia Structural Integrity*, *50*, 184–191. https://doi.org/10.1016/j.prostr.2023.10.040

[16] Bado, M. F., & Casas, J. R. (2021). A review of recent distributed optical fiber sensors applications for civil engineering structural health monitoring. *Sensors*, *21*(5), 1818. https://doi.org/10.3390/s21051818

[17] Jayawickrema, U. M. N., Herath, H. M. C. M., Hettiarachchi, N. K., Sooriyaarachchi, H. P., & Epaarachchi, J. A. (2022). Fibre-optic sensor and deep learning-based structural health monitoring systems for civil structures: A review. *Measurement*, *199*, 111543. https://doi.org/10.1016/j.measurement.2022.111543

[18] Matveenko, V., Kosheleva, N., & Serovaev, G. (2021). Damage detection in materials based on strain measurements. *Acta Mechanica*, *232*(5), 1841–1851. https://doi.org/10.1007/s00707-020-02830-4

[19] Wijaya, H., Rajeev, P., & Gad, E. (2021). Distributed optical fibre sensor for infrastructure monitoring: Field applications. *Optical Fiber Technology*, *64*, 102577. https://doi.org/10.1016/j.yofte.2021.102577

[20] Wu, T., Liu, G., Fu, S., & Xing, F. (2020). Recent progress of fiber-optic sensors for the structural health monitoring of civil infrastructure. *Sensors*, *20*(16), 4517. https://doi.org/10.3390/s20164517

[21] Pereira, J. M. B., Grüner-Nielsen, L., Rottwitt, K., Town, G., Laurell, F., & Margulis, W. (2022). Electrooptic control of the modal distribution in a silicate fiber. *Optics Express*, *30*(8), 12474–12483. https://doi.org/10.1364/OE.453006

[22] Boyd, R. W. (2020). *Nonlinear optics*. USA: Academic Press. https://doi.org/10.1016/C2015-0-05510-1

[23] Jeppesen, P., &Tromborg, B. (2023). *Optical communications from a Fourier perspective. Fourier theory and optical fiber devices and systems*. Netherlands: Elsevier.

[24] Niu, H., Zhang, S., Chen, W., Liu, Y., Li, X., Yan, Y., . . . , & Yuan, L. (2021). Optical fiber sensors based on core-offset structure: A review. *IEEE Sensors Journal*, *21*(20), 22388–22401. https://doi.org/10.1109/JSEN.2021.3110852

[25] Alexeyev, C. N., Barshak, E. V., Lapin, B. P., & Yavorsky, M. A. (2024). Dispersions of robust optical vortices in multihelicoidal fibers with torsional mechanic stress. *Journal of the Optical Society of America B*, *41*(3), 610–616. https://doi.org/10.1364/JOSAB.513654

[26] Polyakova, E. A., Badeeva, E. A., Murashkina, T. I., Badeev, A. V., & Slavkin, I. E. (2020). Influence of optical fiber bends on metrological and operational characteristics of fiber-optic measuring transducers. *Models, Systems, Networks in Economics, Technology, Nature and Society*, *1*(33), 126–135. https://doi.org/10.21685/2227-8486-2020-1-10

[27] Ivanov, S. A., Zakalkin, P. V., & Smirnov, I. Y. (2022). Optical fiber modeling based on phase-loop substitution schemes. *Journal of Communications Technology and Electronics*, *67*(5), 573–580. https://doi.org/10.1134/S1064226922050072

[28] Zhang, Z., Li, R., Wang, C., Zhou, M., Liu, Y., & Pang, Y. (2023). Fusion splicing of hollow-core to standard single-mode fibers using a gradient-index bridge fiber. *Journal of Optical Technology*, *90*(1), 42–45. https://doi.org/10.1364/JOT.90.000042

[29] Melikyants, D. G., Kurlov, V. N., Zaytsev, K. I., & Katyba, G. M. (2023). Bundles of high-refractive-index optical fibers for THz-imaging with subwavelength resolution (Review). *Optics and Spectroscopy*, *131*(6), 720–737. https://doi.org/10.61011/EOS.2023.06.56659.125-23

[30] Adams, M. J. (1981). *An introduction to optical waveguides*. USA: John Wiley & Sons.

[31] Kotlyar V. V., Kovalev A. A., & Nalimov, A. G. (2009). Gradient-index elements of microoptics for superresolution. *Computer Optics*, *33*(4), 369–378.

[32] Gladkikh, V. A., & Vlasenko, V. D. (2021). Investigation of the dependence of the field energy in a low conductive fiber optic with a gradient profile of the refractive index. *Optik*, *245*, 167735. https://doi.org/10.1016/j.ijleo.2021.167735

[33] Gradshtein, I. S., & Ryzhik, I. M. (1971). *Table of integrals, sums, series and products*. USA: Academic Press.

[34] Gladkikh, V. A., & Vlasenko, V. D. (2021). Calculation of splice loss of two fibers, one of which is elliptically deformed along its entire. *Journal of Optical Technology*, *88*(2), 111–115. https://doi.org/10.1364/JOT.88.000111

How to Cite: Vlasenko, V. D., & Gladkikh, V. A. (2024). Study of Dependence of the Energy of the Field in Weakly Conductive Fiberlight-Guide with Gradient Refractive Index Profile Without Regard to Polarization. *Journal of Optics and Photonics Research*. https://doi.org/10.47852/bonviewJOPR42023470